

Mathematical modelling of vehicle drivetrain to predict energy consumption

Latha Ramasamy, Ashok Kumar Loganathan, Rajalakshmi Chinnasamy

Department of Electrical and Electronics Engineering, PSG College of Technology, Coimbatore, India

Article Info

Article history:

Received Nov 25, 2021

Revised May 16, 2022

Accepted Jun 16, 2022

Keywords:

Drivetrain

Energy consumption

Electric vehicles model

Proportional-integral controller

Prediction

ABSTRACT

Nowadays, many firms have started producing electric vehicles (EVs). One of the biggest challenges to broad acceptance of electric vehicles is their limited range EVs. Forecasting future energy usage is one of the way to calculate the driving range. In this paper, a simulation model of the drivetrain has been developed to evaluate the energy flow of a vehicle for the given torque and speed conditions. The energy consumption of an electric vehicle is determined by the vehicle's attributes. Road torque, road speed, motor model, motor controller model, battery model, and PI controller are the primary components of the model. The overall resistive force offered by the vehicle, as well as energy consumption owing to resistive force during motoring and regeneration has been validated through the simulation results. Here, the vehicle model, Mercedes Benz Class C Saloon has been considered.

This is an open access article under the [CC BY-SA](https://creativecommons.org/licenses/by-sa/4.0/) license.



Corresponding Author:

Latha Ramasamy

Department of Electrical and Electronics Engineering, PSG College of Technology

Avinashi Rd, Peelamedu, Coimbatore, Tamil Nadu 641004, India

Email: rla.eee@psgtech.ac.in

1. INTRODUCTION

The vehicle drivetrain system consists of a permanent magnet direct current (PMDC) motor, proportional-integral (PI) based motor controller, and battery. Drivetrain (engine/transmission) efficiency is one of the significant parameters to substantially increase the average fuel economy of the vehicle. In driving cycles, a small percentage of improvement of drivetrain efficiency will improve the reduction in carbon dioxide emissions. In hybrid vehicles, modern drivetrain technologies produce a higher impact on the reduction of engine losses. From the literature, it has been found that each percentage of loss reduction can improve the energy consumption of the vehicle to meet the future emission target. The design of the drivetrain model of the vehicle involves the basic principle of Newton's second law of motion. To model the dynamic behavior of a vehicle, the dynamic equations which describe the physical aspects of the vehicle are required. As per Newton's second law, the net driving force exerted by the vehicle depends on the acceleration of the vehicle.

The vehicle's motion depends on the force produced by the drivetrain of the vehicle which overcomes the resistive forces due to various resistances such as aerodynamic resistance, rolling resistance, gradient resistance, and inertia resistance offered by the vehicle. To know the energy efficiency of driving of internal combustion (IC) engine vehicles, energy consumed to propel the wheels should be determined. Normally IC vehicle has 10% to 25% of energy losses when the power is applied to propel the wheels [1]. The vehicle type, vehicle model, and speed of the vehicle strongly influence the energy consumption of a vehicle. It is a measure to estimate how far a vehicle will travel with the available fuel. According to the estimation of energy consumption and improved configuration of drivetrain technologies, reduction in cost

and reduction in CO₂ emissions can be achieved. Many authors proposed methods to estimate the energy consumption in plug-in hybrid vehicles. Based on real-world measurements an electric vehicle energy consumption models have been built. The energy consumption of electric vehicles (EVs) is usually a variable parameter that depends on other parameters such as road and traffic conditions, driving capability, and temperature. Using detailed values of real-time data three models were constructed to predict the energy consumption for an electric vehicle [2]. A comparison is made between the two versions of Toyota Yaris and claimed that there is a strong reduction in consumption using hybrid vehicles for lower and medium speed and increases its efficiency [3].

The study of driving power estimation for Toyota Prius vehicle proposed a traction force-speed based fuel consumption model. They indicate that the hybrid vehicle driving mode transition is one of the significant parameters which affect energy consumption [4]. The authors describe the process tools such as cost, installation space requirements, weight, the dynamic performance of safety, and efficiency are required for quantitative evaluation of drivetrain concept. Efficiency is one of the most important criteria which determine the overall quality of the drivetrain. All components within the drivetrain are characterized by their efficiency. The power flow of an electric vehicle is investigated to determine the system performance [5], [6]. The study has been done for how the speed factor of the electric motor influences acceleration time along with experimental verification. They developed an algorithm to determine the tractive performance of a designed electric vehicle [7]. Whale optimization algorithm (WOA) is used to optimize the gain parameters of PI controllers and adjust their gains values (K_p and K_i) in correspondence to deviations of EV speed and torque [8]. Energy consumption of the dynamic model of an electric vehicle is examined and the corresponding graph is simulated for the New European Driving Cycle (NEDC) and worldwide harmonized light vehicle test procedure (WLTP) [9]. The vehicle driving range is affected by increased energy consumption at high speeds, large loads, and battery discharge capacity. A study has been carried out to optimize charger selection algorithms, the impact of large loads, and the safety margin for battery discharge [10]-[16]. A comprehensive review of energy consumption is carried out in electrical systems [17]. A simulation model for each of the key components of an electric vehicle such as motor, controller, battery, and drivetrain [18]. A preliminary design has been demonstrated with the use of computer tools [19]. Work focused on the design of the electric propulsion unit and evaluation of the traction motor efficiency maps the drivetrain of the vehicle efficiency of commercially available Honda Insight and Toyota Prius HEVs [20], [21]. Electric vehicle (EV) energy consumption is affected by the traffic environment, terrain, and resistive forces acting on the vehicle, vehicle attributes, and the driver's driving behaviour. With the above unavoidable circumstances, EVs may face a driving safety issue and deteriorates the EV's energy efficiency [22], [23]. The perceived emergence of electric power train noise and its implications were evaluated to prove the responsibilities of the electrified power train [24]. A heuristic technique is also used to reduce electric energy consumption by increasing drivetrain efficiency through component selection [25]. From the literature search, it has been revealed that the automotive industry is still facing design challenges in developing innovative methods to improve drivetrain efficiency. The drivetrain is the core of vehicle technologies. The drivetrain of a vehicle is comprised of a group of components that use the power generated by the engine to move the vehicle. Since the developers are facing difficulty in identifying drivetrain performance and efficiency leads to increasing attention of researchers.

In this paper, a simulation model of the drivetrain has been developed to evaluate the tractive force and energy flow of a vehicle for the given torque and speed conditions. From the calculation, the total resistive force offered by the vehicle and energy consumption due to resistive force during motoring and regeneration has been obtained. So that better reduction of fuel consumption can be obtained and the results will indirectly influence in increasing the driving range of the vehicle.

2. ESTIMATION OF TRACTIVE EFFORT OF THE VEHICLE

During driving, resistive forces act on the vehicles. The electric vehicle motion on an inclined surface is based on resistive forces like an aerodynamic drag force, tire rolling climbing resistance forces and inertia resistance force, and vehicle velocity. The road load resistance values are calculated based on the vehicle specification. Figure 1 shows the schematic of the vehicle. In this paper, the vehicle model, Mercedes Benz Class C Saloon has been considered. The specifications of the vehicle are given in Table 1.

2.1. Aerodynamic drag resistance

The resistance offered by air in the atmosphere as the vehicle passes through it is known as aerodynamic drag. It can be of two forms, drag on the surface of the body due to frontal area and skin friction. Owing to the formation of two pressure areas, aerodynamic drag exerts opposite force as the vehicle moves through the air. The high-pressure zone is created at the front of the vehicle and the low-pressure zone is created at the back of the vehicle. These pressure zones exert force against the vehicle's motion. The

friction of the skin is caused by the contact of moving air with the external part of the vehicle. The shape of the drag plays the main part of aerodynamic drag as opposed to the skin friction of approximately 90 percent of the vehicle’s overall dynamic drag. The mathematical relation of aerodynamic drag is specified in (1).

$$F_{AR} = \frac{1}{2} \rho * A * C_d * (V \pm V_w)^2 \tag{1}$$

Here + for head wind and - for the tail wind, where ρ is air density which defines the resistance force, A is the frontal area of the vehicle, C_d is drag coefficient of the model vehicle, V is the velocity of the model vehicle and V_w is the velocity of the wind. Here the aerodynamic coefficient for the car is taken as 0.3.

Table 1. Specification of the vehicle

S. No	Parameters	Rating
1	Maximum Power	384.87 bhp
2	Maximum Torque	529 Nm at 2500-5000 rpm
3	Gear Box	9
4	Maximum Speed	250 km
5	Weight	1625 kg

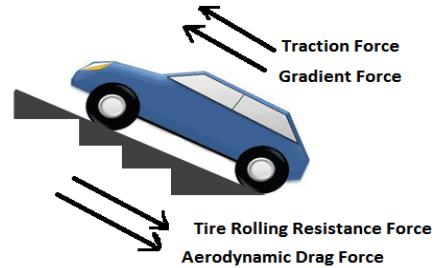


Figure 1. Schematic of the vehicle

2.2. Tire rolling resistance

F_r is the rolling resistance that is created, whenever the vehicle tire deformation occurs. Considering a tire with a perfect circular shape in contact with the road surface, the ground reaction force on the tire falls directly below the wheel axle with no net force to induce any movement. But ideally, at the point of contact, tires are not round but a little flat. Therefore, as the vehicle is going forward, the weight on the wheel and the usual force on the ground results in misalignment. This misalignment leads to the exertion of retarding torque on the wheels by couple forces is known as rolling force resistance, F_r . Rolling resistance force is represented in (2). A pair of retarding forces known as rolling force resistance F_r . As shown in (2) shows the calculation of rolling resistance.

$$F_R = C_r * m * g * \cos \alpha \tag{2}$$

where C_r is road rolling resistance coefficient, m is the mass of the vehicle and g is gravity due to acceleration. The variations of various rolling coefficients for different road surfaces are shown in Table 2.

Table 2. Rolling coefficients for various road surfaces

Road Surface	Road rolling resistance coefficient (C_r)
Concrete or Asphalt	0.013
Small gravel ground	0.02
Macadamized road	0.025
Soil road	0.1-0.35
Road	0.01-0.035

2.3. Gradient resistance

The resistance occurs while the vehicle is moving on the sloping road. The gravity component produces gradient resistance. α shows the direction of the gradient is expressed in degrees. As shown in (3) describes the formula for gradient resistance.

$$F_{GR} = m * g * \sin \alpha \tag{3}$$

where α is the slope angle of the road.

2.4. Inertia resistance

It is the force required to accelerate the vehicle mass at a certain magnitude of acceleration. As shown in (4) and (5) represent inertia force and total force respectively.

$$F_I = m * a \tag{4}$$

$$F_{Total} = F_{AR} + F_R + F_{GR} + F_I \tag{5}$$

2.5. Tractive force

The force used to produce the difference between the tangential force and body to overcome the total resistive force at a given driving condition on tires is called tractive force which can be found using (6). The instantaneous tractive power (P_w) from the drivetrain to sustain a certain speed level is determined by (7). The energy consumption is obtained by integrating the total power over the period for the entire cycle is given in (8).

$$F_{TF} = F_a + F_{Total} \tag{6}$$

$$P_W = F_{TF} * V \tag{7}$$

$$E_T = \int P_W dt \tag{8}$$

In the drivetrain, electric motor energy efficiency tightly linked to the resistive force of the vehicle.

3. MODELLING OF ELECTRIC VEHICLE DRIVETRAIN

A speed-torque map of conventional four-quadrant operation is shown in Figure 2. In an inclined surface, the vehicle is operated in two modes such as motoring and braking mode. If speed and torque have the matching polarity, then power is transferred from the engine to the load and the vehicle is operated in motoring mode and supporting its motion.

Furthermore, if the speed is positive and the torque is negative and vice versa, the outside mechanical force drives the motor, which results in the transfer of energy back to the battery and the vehicle is operated in regenerative mode and results in opposes the motion. During motoring as well as in braking mode, the vehicle is moving in both forward and reverse directions according to the conventions about the signs of torque and speed of the vehicle. A battery controller monitors the parameters of the main batteries and controls the battery pack. The schematic of the vehicle drivetrain is shown in Figure 3. The model can be used to calculate the energy flow of the drivetrain and determine the ability of the system for specific torque and speed requirements. The model consists of components such as motor model, motor controller, battery, and PI controller. The speed and torque values are given to the motor model which converts the speed and torque values into voltage and current. The voltage follows the speed and the current follows the torque. The motor model output is fed into the motor controller for the high-low transition of values which is given to the battery model. The battery has an internal resistance and is modeled as a voltage source. Internal power loss in the battery's resistance is factored into the model. The model does not include a time lag component. The battery model calculates the required battery's internal voltage using current and voltage information from the Motor Controller. In a battery model, the battery voltage error is obtained based on the comparison of actual battery voltage with the calculated battery voltage.

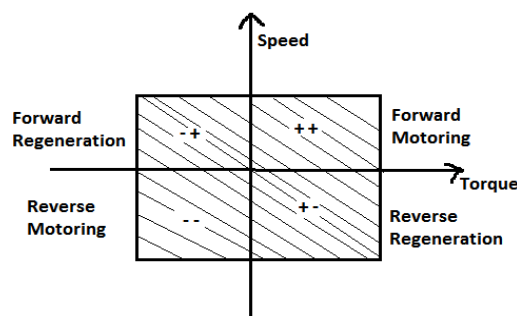


Figure 2. Four quadrant vehicle operation

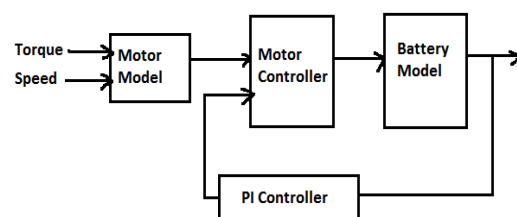


Figure 3. Schematic of vehicle drivetrain

The error voltage is given to the PI controller for tuning to improve the drive train efficiency. Evaluation of the longitudinal nature of electric vehicles is described by the governing (9) to (16) of the drivetrain system of the vehicle [6]. Developed motor torque (T_{dev}) is proportional to the current in the armature (I_{arm}). Developed motor voltage (V_{dev}) is proportional to the speed of the armature (ω_d).

$$T_{dev} = K_m * I_{arm} \quad (9)$$

$$V_{dev} = \omega_d * K_m \quad (10)$$

where K_m is motor constant.

3.1. Motor equations

The terminal voltage of the high-side of the motor (V_H) is:

$$V_H = I_H * R_a + L_H \frac{di}{dt} + V_{dev} \quad (11)$$

where I_H , L_H are the current and inductor at the high side of the motor. The motor controller is used to maintain the same input and output power. Voltage and current at the input of the motor controller are represented as in (12) and (13) respectively.

$$V_H = K * V_L \quad (12)$$

$$I_H = \frac{1}{K} * I_L \quad (13)$$

Where V_L and I_L are voltage and current at the output of the motor controller respectively. Here the voltage source E_B and internal power loss due to battery resistance R_B are modeled as a battery.

$$V_L = I_L * R_B + E_B \quad (14)$$

The battery error has been obtained from the difference between calculated battery voltage and actual battery voltage. The error (B_{err}) is used to calculate the gain of the PI controller.

$$B_{err} = E_{B(actual)} - E_{B(calculated)} \quad (15)$$

$$K = (K_p + s * K_i) * B_{err} \quad (16)$$

4. SIMULATION MODEL AND RESULTS

Specifications of the vehicle are given in Table 3. To describe the energy consumption of the Mercedes Benz Class C Saloon hybrid vehicle model is simulated using MATLAB/Simulink as shown in Figure 4. In the simulation, a lookup table is framed for the speed and torque data. The data represents speed-time and torque-time values which correspond to the transition time of the speed and torque curves. Depending on the road characteristics speed values are assumed and from the wheel power corresponding torque is calculated.

Table 3. Key vehicle data specifications

Parameters	Values
Drag coefficient	0.26
Density (kg/m ³)	1.225
Frontal area (m ²)	2.20
Velocity (m/s)	1.25
Gravity (m/s ²)	1.8
Mass(kg)	1625

Speed values=[0 2000 5000 1000 2000]

Speed time=[0 20 50 85 100]

Torque values=[0 550 330 160 -220 130 0]

Torque time=[0 10 20 40 55 80 100]

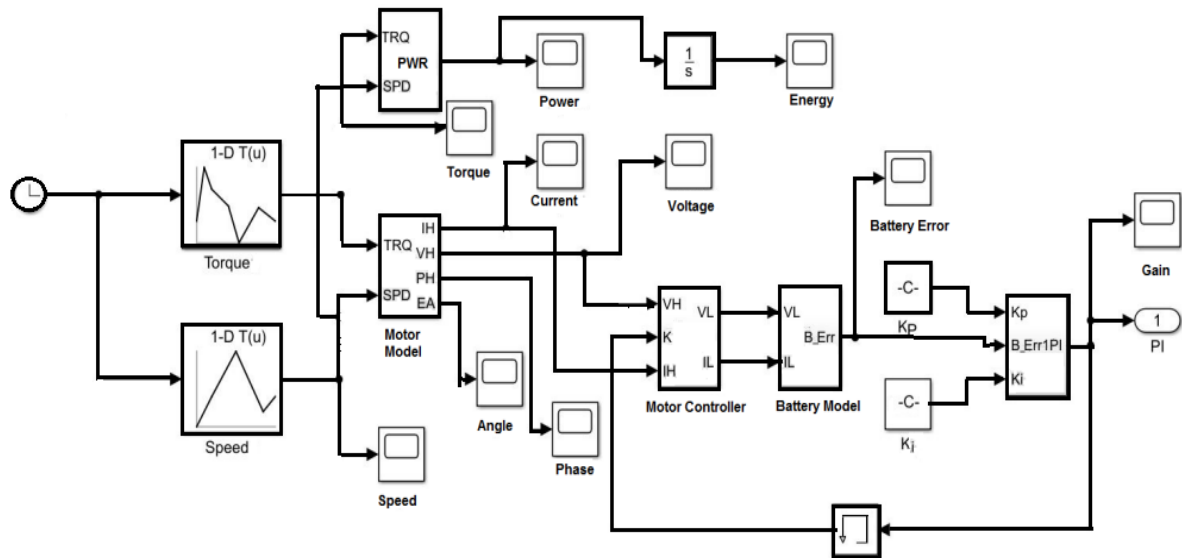


Figure 4. Simulation model of vehicle drivetrain

A traditional 4-quadrant speed-torque map displays +/-Speed on the x-axis, and +/-Torque on the y-axis. If speed and torque have the same polarity then power is transferred from the engine to the load, and the engine is operating in motoring mode. Furthermore, if the speed is positive and the torque negative, the outside mechanical force drives the motor, which results in the transfer of energy back to the battery. Figure 5 and Figure 6 show the analysis of the voltage and current variations of the motor based on the acceleration or based on the driving cycles. For positive values of both current and voltage, the torque given by the vehicle in the rotating direction and power is transferred to charge the battery. However, if the current is in the opposite polarity at T=50 seconds, then the vehicle is driven back and it functions as a generator with reverse current flow.

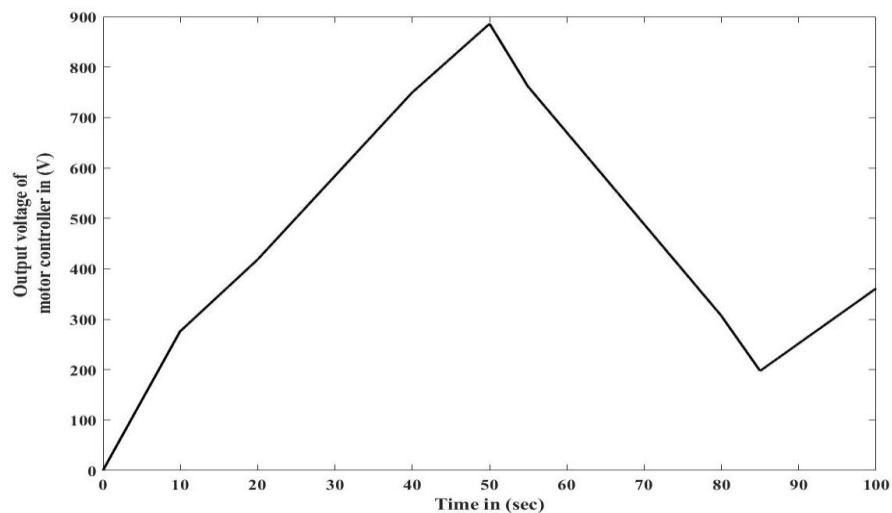


Figure 5. Voltage of motor controller

The simulation model modifies the proportional and integral constants K_p and K_i to satisfy the demands of driving torque. The simulation output as shown in Figure 7, is obtained by comparing the actual battery voltage E_B with a calculated voltage of the battery $E_{B(calculated)}$. The battery voltage error is positive during motoring mode till T=50 seconds and it becomes negative during the regenerative mode. The largest negative value of battery error of -200 V at 0 sec occurs at the initial stage of the simulation due to natural response which is normally ignored. The magnitude of the PI controller's input and output will be affected by

this voltage variation. The error output is used as input to the PI controller. During motor starting, the controller quickly recovers the system and compensates for the maximum deviation of around 25 V. The controller's performance is satisfactory because the error is almost zero. However, employing other intelligent methods, the controller performance would still be enhanced. As seen in Figure 8, the value of controller gain K fluctuates according to the speed demand, where the value of K rises as the speed demand rises. The integrator in the PI controller block is configured during modeling. To avoid an algebraic loop error during simulation, the integrator in the PI controller block is set to 0.1 at the beginning during modeling. The controller gain increases during the motoring mode and decreases during the regenerative mode.

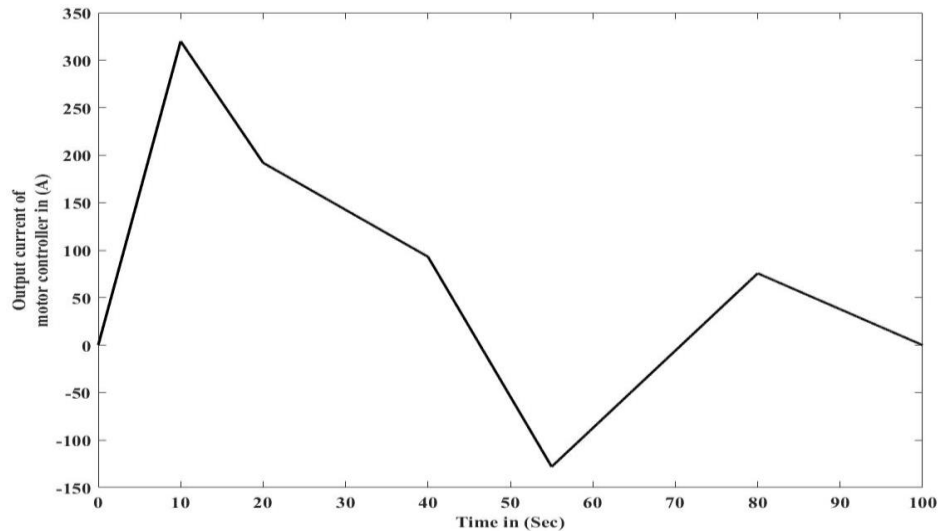


Figure 6. Current output of motor controller

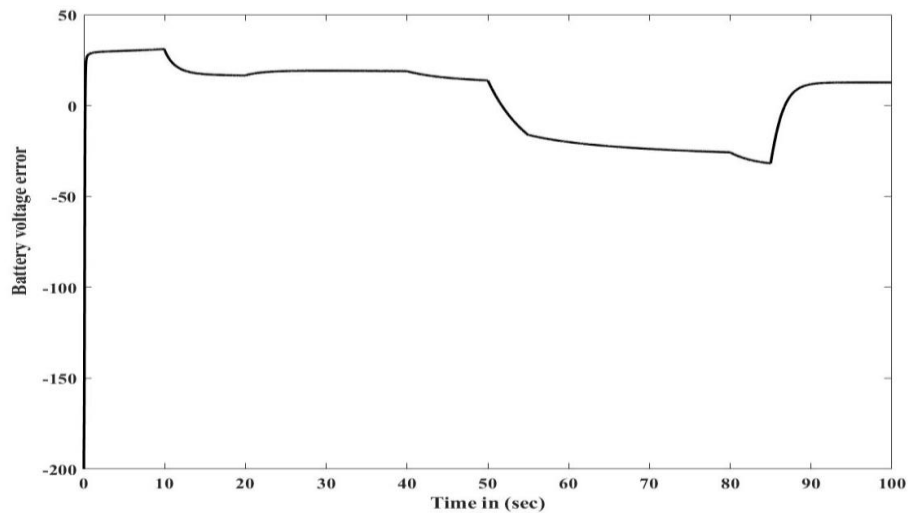


Figure 7. Battery voltage error

During an instant of the driving cycle, the energy consumed by the vehicle has been obtained by adjusting the gain. The PI controller generates an error correction signal which is directly proportional to the signal error and proportional to the integral of an error signal. The proportional signal allows the controller to respond to system change and the integral signal allows by integrating the signal over time to reduce constant errors. The constants K_p and K_i of the controller are calculated by trial and error, and the tuning process was simply a change of the values while monitoring the magnitude of the B_{err} signal. As shown in Figure 8, the

average value of the gain K is 4.0. From the simulation results, it has been observed that the battery of the electric vehicle provides enough electric power to overcome the speed and torque produced by the vehicle. The EV's performance depends on the performance of the controller to compensate for the voltage error.

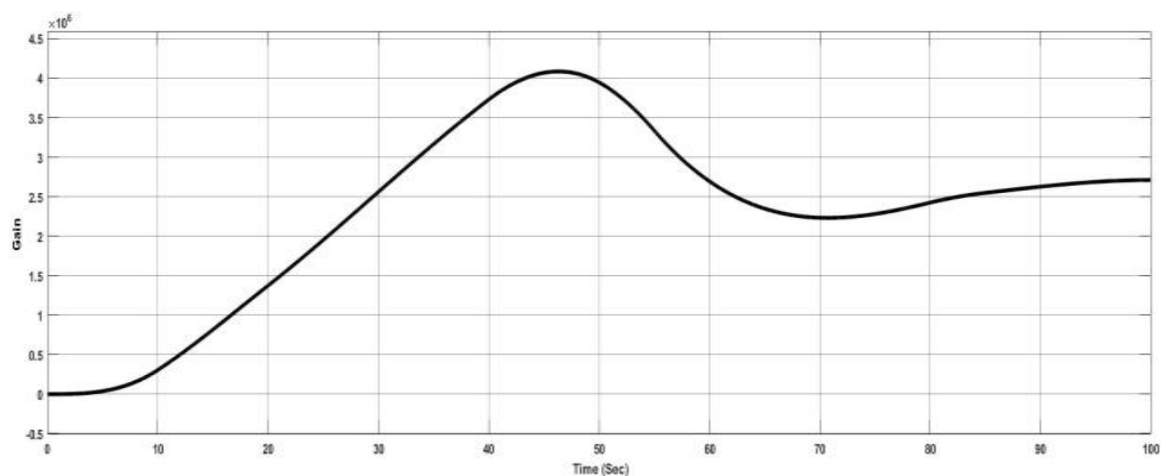


Figure 8. Controller gain

5. CONCLUSION

In this paper, the road load resistance is calculated for the Mercedes Benz Class C Saloon vehicle, and analysis of energy flow in motoring and regeneration operations of the vehicle is simulated using MATLAB/Simulink. Normally prototyping and testing are costly and complex activities, so automobile designers depend largely on modeling and simulation to determine the optimum energy control strategy and precise component size, as well as to reduce energy consumption. In this paper, mathematical models of drive components of the vehicle are developed to enable the perfect understanding of the flow of energy. Depending on the sign of the total energy, we can easily distinguish the acceleration and deceleration phases of the vehicle. The voltage, current, and power at each instant of simulation are obtained to analyze the energy flow of the drivetrain. Optimum ratings of power and torque, less fuel consumption, and increased battery life can be obtained with proper maintenance of the flow of energy. The observed results indirectly influence the increase in the driving range of the vehicle. In the future, the proposed model will serve as a foundation for the further development of EVs.

REFERENCES

- [1] Ed Pike, *Opportunities to Improve Tire Energy Efficiency*. White Paper, 2011.
- [2] C. D. Cauwer, J. V. Mierlo, and T. Coosemans, "Energy consumption prediction for electric vehicles based on real-world data," *Energies*, vol. 8, no. 8, pp. 8573–8593, Aug. 2015, doi: 10.3390/en8088573.
- [3] F. Orecchini *et al.*, "Energy consumption of a last generation full hybrid vehicle compared with a conventional vehicle in real drive conditions," *Energy Procedia*, vol. 148, pp. 289–296, Aug. 2018, doi: 10.1016/j.egypro.2018.08.080.
- [4] S. Pitanuwat, H. Aoki, S. Iizuka, and T. Morikawa, "Development of hybrid vehicle energy consumption model for transportation applications-Part II: Traction force-speed based energy consumption modeling," *World Electric Vehicle Journal*, vol. 10, no. 2, p. 22, May 2019, doi: 10.3390/wevj10020022.
- [5] M. Felden, P. Bütterling, P. Jeck, L. Eckstein, and K. Hameyer, "Electric vehicle drive trains: From the specification sheet to the drive-train concept," in *Proceedings of EPE-PEMC 2010 - 14th International Power Electronics and Motion Control Conference*, Sep. 2010, doi: 10.1109/EPEPEMC.2010.5606531.
- [6] D. McDonald LSSU Sault Ste Marie, "Electric Vehicle Drive Simulation LSSU with MATLAB/Simulink," in *Proceedings of the 2012 North-Central Section Conference*, 2012.
- [7] M. Sapundzhiev, I. Evtimov, and R. Ivanov, "Determination of the needed power of an electric motor on the basis of acceleration time of the electric car," *IOP Conference Series: Materials Science and Engineering*, vol. 252, no. 1, p. 012063, Oct. 2017, doi: 10.1088/1757-899X/252/1/012063.
- [8] C. H. Kim and K. M. Lee, "Analytical study on the performance analysis of power train system of an electric vehicle," *World Electric Vehicle Journal*, vol. 3, no. 4, pp. 830–836, Dec. 2009, doi: 10.3390/wevj3040830.
- [9] S. Kaushik, "Modeling and simulation of electric vehicle to optimize its cost and range," *International Journal of Engineering and Advanced Technology*, vol. 8, no. 6, pp. 415–419, Aug. 2019, doi: 10.35940/ijeat.E7819.088619.
- [10] A. O. Kiyaklı and H. Solmaz, "Modeling of an electric vehicle with MATLAB/Simulink," *International Journal of Automotive Science And Technology*, pp. 9–15, Jan. 2019, doi: 10.30939/ijastech.475477.
- [11] G. Wager, J. Whale, and T. Braunl, "Driving electric vehicles at highway speeds: The effect of higher driving speeds on energy consumption and driving range for electric vehicles in Australia," *Renewable and Sustainable Energy Reviews*, vol. 63, pp. 158–165, Sep. 2016, doi: 10.1016/j.rser.2016.05.060.

- [12] T. C. Moore, "Tools and Strategies for Hybrid-Electric Drive system Optimization," *SAE Transactions*, vol. 105, no. 6, pp. 1515–1532, 1996.
- [13] R. Farrington and J. Rugh, "Impact of vehicle air-conditioning on fuel economy, tailpipe emissions, and electric vehicle range," *Earth Technologies Forum*, Washington, 2000. [Online]. Available: <http://www.smesfair.com/pdf/airconditioning/28960.pdf>
- [14] T. Yuksel and J. J. Michalek, "Effects of regional temperature on electric vehicle efficiency, range, and emissions in the united states," *Environmental Science and Technology*, vol. 49, no. 6, pp. 3974–3980, Mar. 2015, doi: 10.1021/es505621s.
- [15] M. G. Vayá, "Optimizing the electricity demand of electric vehicles: creating value through flexibility," Ph.D. dissertation, ETH Zurich, 2015.
- [16] S. N. Yang, W. S. Cheng, Y. C. Hsu, C. H. Gan, and Y. B. Lin, "Charge scheduling of electric vehicles in highways," *Mathematical and Computer Modelling*, vol. 57, no. 11–12, pp. 2873–2882, Jun. 2013, doi: 10.1016/j.mcm.2011.11.054.
- [17] S. Khan and M. Saini, "A comprehensive study on energy meters and power tampering attempts," *International Journal of Applied Power Engineering (IJAPE)*, vol. 10, no. 4, p. 315, Dec. 2021, doi: 10.11591/ijape.v10.i4.pp315-325.
- [18] I. Husain and M. S. Islam, "Design, modeling and simulation of an electric vehicle system," in *SAE Technical Papers*, Mar. 1999, doi: 10.4271/1999-01-1149.
- [19] E. A. Grunditz, "Design and assessment of battery electric vehicle powertrain, with respect to performance, energy consumption and electric motor thermal capability," Ph.D. dissertation, Chalmers University of Technology, Sewden, 2016.
- [20] S. S. Williamson, S. M. Lukic, and A. Emadi, "Comprehensive drive train efficiency analysis of hybrid electric and fuel cell vehicles based on motor-controller efficiency modeling," *IEEE Transactions on Power Electronics*, vol. 21, no. 3, pp. 730–740, May 2006, doi: 10.1109/TPEL.2006.872388.
- [21] P. B. Bhaskar, S. Deshmukh, P. Khannan, and A. Shaik, "Recent trends on drivetrain control strategies and battery parameters of a hybrid electric vehicle," in *SAE Technical Papers*, Oct. 2019, no. October, doi: 10.4271/2019-28-0155.
- [22] J. P. Phatak, L. Venkatesha, and C. S. Raviprasad, "Driving cycle based battery rating selection and range analysis in EV applications," *International Journal of Power Electronics and Drive Systems (IJPEDS)*, vol. 12, no. 2, p. 637, Jun. 2021, doi: 10.11591/ijpeds.v12.i2.pp637-649.
- [23] X. Zhou, F. Sun, C. Zhang, and C. Sun, "Stochastically predictive co-optimization of the speed planning and powertrain controls for electric vehicles driving in random traffic environment safely and efficiently," *Journal of Power Sources*, vol. 528, p. 231200, Apr. 2022, doi: 10.1016/j.jpowsour.2022.231200.
- [24] M. Munder and C. C. Carbon, "Howl, whirr, and whistle: The perception of electric powertrain noise and its importance for perceived quality in electrified vehicles," *Applied Acoustics*, vol. 185, p. 108412, Jan. 2022, doi: 10.1016/j.apacoust.2021.108412.
- [25] S. Chakraborty *et al.*, "Multiobjective GA optimization for energy efficient electric vehicle drivetrains," in *2021 16th International Conference on Ecological Vehicles and Renewable Energies, EVER 2021*, May 2021, pp. 1–7, doi: 10.1109/EVER52347.2021.9456619.

BIOGRAPHIES OF AUTHORS



Latha Ramasamy    is Associate Professor in the department of Electrical and Electronics Engineering, PSG College of Technology, Coimbatore, India where she has been a faculty member since 2007. She graduated in Electrical and Electronics Engineering from Bharathiyar University, India, ME in Power Systems Engineering and PhD in Electrical Engineering from Anna University, Chennai. Her current research interests include microgrids, renewable energy systems, power system control, energy management systems, power electronic drives and electric vehicles. She has supervised more than 20 masters students and supervising 6 PhD students. She can be contacted at email: rla.eee@psgtech.ac.in.



Ashok Kumar Loganathan    completed his graduate in Electrical and Electronics Engineering from University of Madras, India and his post-graduation in Electrical Machines from PSG College of Technology and Masters in Business administration from IGNOU, New Delhi. He completed his PhD in the field of Wearable Electronics from Anna University, Chennai. He is a post doctoral Research Fellow from San Diego State University, California. His current research focuses on Integration of Renewable Energy Systems in the Smart grid and Wearable Electronics. He has published 170 technical papers and 9 books. He has received project worth of Rs.3.5 Crores from various funding agencies. Presently he is working as Professor in the department of EEE, PSG College of Technology. He can be contacted at email: lak.eee@psgtech.ac.in.



Rajalakshmi Chinnasamy    is currently working as an Associate Software Engineer in Bosch Global Software Technology, coimbatore since 2021. She has graduated in Electrical and Electronics Engineering under Anna University, Chennai and M.E in Power Electronics and Drives in PSG College of Technology, Coimbatore. Her current research interests in vehicle dynamics, power train, and driver assistant system technology. She can be contacted at email: radhika.raji97@gmail.com.